Journal of Molecular Structure 1272 (2023) 134171

Contents lists available at ScienceDirect

Journal of Molecular Structure

journal homepage: www.elsevier.com/locate/molstr

Novel thiadiazol derivatives; design, synthesis, biological activity, molecular docking and molecular dynamics

Derya Osmaniye[a,b,*], Asaf Evrim Evren[a,c], Şevval Karaca[d], Yusuf Özkay[a,b], Zafer Asım Kaplancıklı[a,*]

[a] Department of Pharmaceutical Chemistry, Faculty of Pharmacy, Anadolu University, 26470 Eskişehir, Turkey
[b] Central Analysis Laboratory, Faculty of Pharmacy, Anadolu University, 26470 Eskişehir, Turkey
[c] Pharmacy Services, Vocational School of Health Services, Bilecik Şeyh Edebali University, Bilecik 11230, Turkey
[d] Department of Biochemistry, Faculty of Pharmacy, Anadolu University, 26470 Eskişehir, Turkey

ARTICLE INFO

Article history:
Received 13 May 2022
Revised 16 August 2022
Accepted 17 September 2022
Available online 18 September 2022

Keywords:
Thiadiazol
Selective COX-2 inhibition
Molecular docking
Molecular dynamics

ABSTRACT

Currently, selective COX-2 inhibitors are used as a novel alternative approach in the course of pain management due to their reduced adverse that generally occur after COX-1 inhibition by non-selective COX inhibitors. In this work, 16 new thiadiazole derivatives (**3a-3p**) were designed, synthesized and biologically evaluated for their COX-1 and COX-2 inhibitory potential using the *in vitro* fluorometric method. The biological evaluation showed that compounds **3c** and **3d** displayed significant activity against COX-2 with IC_{50} values of 0.350±0.015 μM and 0.134±0.004 μM, respectively, making the compound **3d** similar in its activity to the reference drug celecoxib (IC_{50}=0.132±0.005 μM). Further docking simulation also revealed that the most active derivative (**3d**) interacted with the enzyme active site in a similar manner to celecoxib. The binding modes of the compound on COX-2 were fully elucidated by molecular dynamics studies.

1. Introduction

Inflammation, which can be used as a target for anti-inflammatory therapy, is a complex process involving various enzymes [1]. It is known that long-term treatment with NSAIDs, which suppresses the release of prostaglandins (PGs) and thromboxane (TxA) by inhibiting the cyclooxygenase isoforms cyclooxygenase-1 (COX-1) and COX-2 as the primary mechanism of action, causes serious adverse effects in the GI tract. These undesirable effects arise from undesired inhibition of COX-1, resulting in dramatic reductions in gastroprotective PG levels [2]. The therapeutic utility of non-selective NSAIDs have been limited by their frequent gastrointestinal side effects, because they suppress inflammation by inhibiting prostaglandin biosynthesis from arachidonic acid precursors by blocking COX isozymes [3]. Non-selective NSAIDs are clinically used under certain limitations, especially in patients with a history of peptic ulcers, because of the accompanying primary and secondary adverse effects [4]. Selective COX-2 inhibitors, which have no effect on the synthesis of prostaglandins in the gastric mucosa, do not cause acute damage or chronic ulcers. This advantage also proposes the treatment of inflammation with the selective inhibitory effect of COX-2 to the clinic as safer anti-inflammatory agents [5–11].

Each monomer of COX contains a separate cyclooxygenase and peroxidase active site that is functionally linked by a bridging heme moiety. For prostaglandin H_2 production, arachidonic acid binds within the cyclooxygenase channel with both the carboxylate moiety near Arg120 and Tyr355 at the channel entrance and the ω-terminus in a hydrophobic groove on the side chain of Ser530 adjacent to Gly533 on which it is based [12]. In addition, the helix of the membrane-binding domain is positioned differently in COX-2 shifting the position of Arg120 in the contraction region, and thus provides a larger solvent accessible surface at the interface between the membrane-binding domain and COX-2 active site compared to COX-1. This single difference acquires a small side hydrophobic pocket in COX-2, which has proven important in binding some COX-2 selective inhibitors [13,14]. Most COX-2 selective drugs include a core ring with two aromatic rings, either homocyclic or heterocyclic groups, connected to adjacent atoms . One of these aryl groups has a methyl (SO_2CH_3) or amino (SO_2NH_2) sulfonyl group added to the para position in order to increase selectivity targeting the hydrophobic pocket [15]. It was revealed that similar to the sulfonamide moiety, the methyl sulfonyl group of rofecoxib is located in the side pocket due to interacting with the amino acids His90 and Arg513 (hydrophilic) positioned at the base of the side pocket within the COX channel [1]. However, due to

* Corresponding authors at: Anadolu University, Faculty of Pharmacy, Department of Pharmaceutical Chemistry, 26470, Eskişehir, Turkey.
E-mail address: dosmaniye@anadolu.edu.tr (D. Osmaniye).

https://doi.org/10.1016/j.molstruc.2022.134171
0022-2860/

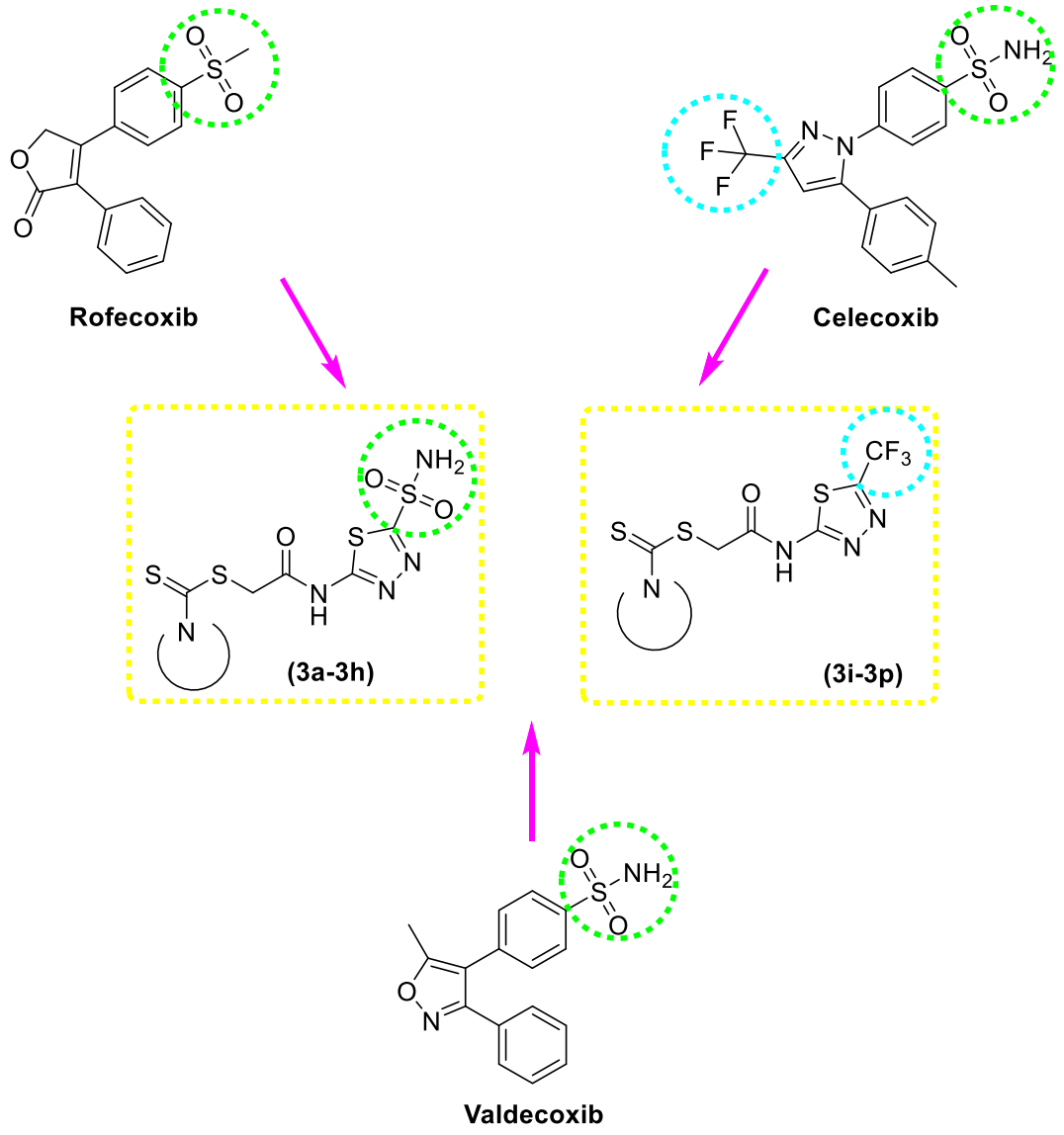

Fig. 1. Some representative examples of selective COX-2 inhibitors (celecoxib, rofecoxib, valdecoxib) and the designed compounds 3a-3p.

an increased risk of cardiovascular symptoms, this drug was withdrawn from the market. Compared to celecoxib, selective COX-2 inhibitors that contain sulfonamides appear to be a promising topic for research in recent studies [11,16–23].

In this study, new thiadiazol derivatives containing sulfonamide or trifluoromethyl structure were designed. The trifluoromethyl group, a group that is found in the structure of celecoxib, was selected due to its large size and ability to be inserted into the hydrophobic pocket therefore its contribution to the activity was investigated. It is also expected that sulfonamide structure are able to fit into the hydrophobic pocket providing COX-2 selectivity. More flexible structures are preferred for other parts of the molecule. It is thought that the obtained small molecules will be effective in selective COX-2 inhibition Fig. 1.

2. Experimental

2.1. Chemistry

All the chemicals used in the synthesis were obtained from Merck (Darmstadt, Germany) or Sigma-Aldrich (St. Louis, MO, USA). A MP90 digital melting point apparatus (Mettler Toledo, OH, USA) was used to determine the melting points of the resulting compounds and was presented uncorrected. ^{1}H NMR and ^{13}C NMR spectra were recorded by a Bruker 300 MHz and 75 MHz digital FT-NMR spectrometer (Bruker Bioscience, Billerica, MA, USA) in DMSO–d_6, respectively. In the NMR spectra, splitting patterns were determined and recognized as follows: s: singlet, d: doublet, t: triplet, dd: double doublet, and m: multiplet. Coupling constants (J) were reported in units of Hertz (Hz). Mass spectra were recorded on an LCMS-IT-TOF (Shimadzu, Kyoto, Japan) by means of the ESI method. Silica gel 60 F254 with thin-layer chromatography (Merck KGaA, Darmstadt, Germany) was used to check the purity of compounds.

2.1.1. General procedure for the synthesis of the compounds

2.1.1.1. Synthesis of 2-chloro-N-(5-sulfamoyl-1,3,4-thiadiazol-2-yl)acetamide/2-chloro-N-(5-(trifluoromethyl)−1,3,4-thiadiazol-2-yl)acetamide (1a-1b). 5-amino-1,3,4-thiadiazol-2-sulfonamide (0.019 mol) was dissolved in DMF. 2-Chloroacetyl chloride solution in DMF was added as dropwise in reaction mixture. The reaction was processed under magnetic stirring for 10 h. After completion of the reaction, the mixture was poured on an ice-bath, precipitated product was filtered, dried, and recrystallized from EtOH.

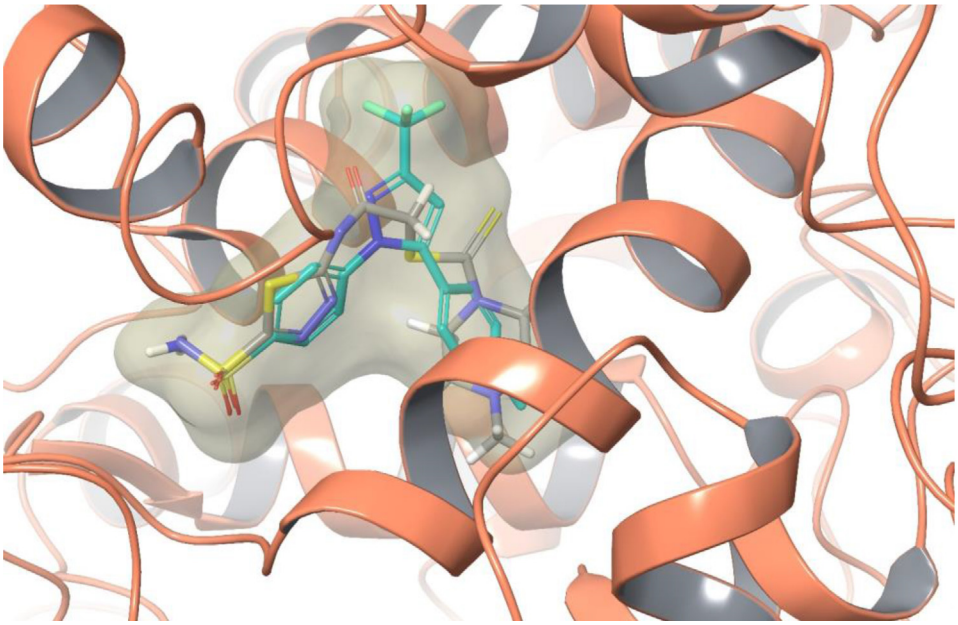

Fig. 2. The superimposition poses of celecoxib and compound 3d in the enzyme active site (PDB Code: 6COX).

Beside, 5-(trifluoromethyl)−1,3,4-thiadiazol-2-amine (0.019 mol) was dissolved in THF. TEA was used as catalyst. 2-Chloroacetyl chloride solution in THF was added as dropwise onto reaction mixture. The reaction was processed under magnetic stirring for 10 h. After completion of the reaction the THF removed using rotavapor. The precipitated product was washed with water, dried, and recrystallized from EtOH.

2.1.1.2. Synthesis of dithiocarbamate salts (2a-2 h). Secondary amine derivatives were dissolved in absolute ethanol (10 mL) and an equimolar quantity of a NaOH was added to the reaction mixture. The carbon disulfide solution in EtOH was added to the reaction mixture as dropwise. After completion of the reaction the precipitated product was filtered washed with diethyl ether 3 times.

2.1.1.3. General procedures of target compounds (3a-3p). The compounds **2a**–2 h (1 mmol) and dithiocarbamate salts (**2a-**2 h) (1 mmol) were stirred in acetone (20 mL) until all the starting compounds disappeared, as determined by TLC. After completion of the reaction the acetone removed using rotavapor. The precipitated product was washed with water, dried, and recrystallized from EtOH.

*2-oxo-2-((5-sulfamoyl-1,3,4-thiadiazol-2-yl)amino)ethyl pyrrolidine-1-carbodithioate (**3a**)*

Yield: 83%, M.P.: 220.8–222.3 °C. ^{1}H NMR (300 MHz, DMSO–d_6): δ = 1.90–1.95 (2H, m, pyrrolidine), 2.03–2.08 (2H, m, pyrrolidine), 3.68 (2H, t, J = 6.8 Hz, pyrrolidine), 3.74 (2H, t, J = 6.8 Hz, pyrrolidine), 4.43 (2H, s, -CH_2-), 8.36 (2H, s, -SO_2NH_2), 13.37 (1H, s, -NH). ^{13}C NMR (75 MHz, DMSO–d_6): δ =24.31, 26.21, 51.21, 55.78, 161.71, 164.86, 167.83, 189.94. HRMS (*m/z*): $[M + H]^+$ calcd for $C_9H_{13}N_5O_3S_4$: 367.9974; found 367.9959.

*2-oxo-2-((5-sulfamoyl-1,3,4-thiadiazol-2-yl)amino)ethyl piperidine-1-carbodithioate (**3b**)*

Yield: 79%, M.P.: 195.3–196.8 °C. ^{1}H NMR (300 MHz, DMSO–d_6): δ = 1.64 (6H, br.s., piperidine), 3.93 (2H, br.s., piperidine), 4.18 (2H, br.s., piperidine), 4.43 (2H, s, -CH_2-), 8.35 (2H, s, -SO_2NH_2), 13.37 (1H, s, -NH). ^{13}C NMR (75 MHz, DMSO–d_6): δ =23.86, 25.62, 26.30, 51.74, 53.11, 161.77, 164.82, 167.91, 192.83. HRMS (*m/z*): $[M+Na]^+$ calcd for $C_{10}H_{15}N_5O_3S_4$: 403.9950; found 403.9961.

*2-oxo-2-((5-sulfamoyl-1,3,4-thiadiazol-2-yl)amino)ethyl 4-methylpiperidine-1-carbodithioate (**3c**)*

Yield: 79%, M.P.: 192.3–194.5 °C. ^{1}H NMR (300 MHz, DMSO–d_6): δ = 0.93 (3H, d, J = 6.1 Hz, -CH_3), 1.12–1.14 (2H, m, piperidine), 1.71–1.81 (3H, m, piperidine), 3.16–3.24 (1H, m, piperidine), 3.41–3.45 (1H, m, piperidine), 4.48 (2H, s, -CH_2-), 4.49 (1H, br.s., piperidine), 5.15–5.19 (1H, m, piperidine), 8.35 (2H, s, -SO_2NH_2), 13.37 (1H, s, -NH). ^{13}C NMR (75 MHz, DMSO–d_6): δ =21.50, 30.34, 33.61, 34.23, 50.84, 52.36, 161.74, 164.85, 167.88, 192.96. HRMS (*m/z*): $[M + H]^+$ calcd for $C_{11}H_{17}N_5O_3S_4$: 396.0287; found 396.0273.

*2-oxo-2-((5-sulfamoyl-1,3,4-thiadiazol-2-yl)amino)ethyl 4-methylpiperazine-1-carbodithioate (**3d**)*

Yield: 83%, M.P.: 174.5–176.3 °C. ^{1}H NMR (300 MHz, DMSO–d_6): δ = 2.39 (3H, s, -CH_3), 2.71 (4H, br.s., piperazine), 4.05 (2H, br.s., piperazine), 4.45 (2H, s, -CH_2-), 8.35 (2H, s, -SO_2NH_2). ^{13}C NMR (75 MHz, DMSO–d_6): δ =42.96, 44.46, 51.46, 53.57, 161.82, 164.82, 167.75, 194.96. HRMS (*m/z*): $[M + H]^+$ calcd for $C_{10}H_{16}N_6O_3S_4$: 397.0239; found 397.0246.

*2-oxo-2-((5-sulfamoyl-1,3,4-thiadiazol-2-yl)amino)ethyl 4-ethylpiperazine-1-carbodithioate (**3e**)*

Yield: 79%, M.P.: 139.9–142.1 °C. ^{1}H NMR (300 MHz, DMSO–d_6): δ = 1.05 (3H, t, J = 7.2 Hz, -CH_3), 2.47–2.52 (2H, m, -CH_2-), 2.62 (4H, br.s., piperazine), 4.00 (2H, br.s., piperazine), 4.22 (2H, br.s., piperazine), 4.44 (2H, s, -CH_2-), 8.34 (2H, s, -SO_2NH_2). ^{13}C NMR (75 MHz, DMSO–d_6): δ =11.80, 43.19, 49.73, 50.96, 51.36, 51.74, 162.02, 164.71, 167.88, 194.55. HRMS (*m/z*): $[M + H]^+$ calcd for $C_{11}H_{18}N_6O_3S_4$: 411.0396; found 411.0397.

*2-oxo-2-((5-sulfamoyl-1,3,4-thiadiazol-2-yl)amino)ethyl 4-(methylsulfonyl)piperazine-1-carbodithioate (**3f**)*

Yield: 80%, M.P.: 181.6–183.9 °C. ^{1}H NMR (300 MHz, DMSO–d_6): δ = 2.94 (3H, s, -CH_3), 3.27 (4H, br.s., piperazine), 4.10 (2H, br.s., piperazine), 4.30 (2H, br.s., piperazine), 4.44 (2H, s, -CH_2-), 8.29 (2H, s, -SO_2NH_2). ^{13}C NMR (75 MHz, DMSO–d_6): δ =34.84, 40.64, 45.35, 49.87, 50.85, 162.63, 164.43, 168.06, 195.44. HRMS (*m/z*): $[M + H]^+$ calcd for $C_{10}H_{16}N_6O_5S_5$: 460.9858; found 460.9870.

*2-oxo-2-((5-sulfamoyl-1,3,4-thiadiazol-2-yl)amino)ethyl 4-(ethylsulfonyl)piperazine-1-carbodithioate (*3 g*)*

Yield: 77%, M.P.: 180.1–182.7 °C. ^{1}H NMR (300 MHz, DMSO–d_6): δ = 1.21 (3H, t, J = 7.36 Hz, -CH_3), 3.11 (2H, q, J = 7.4 Hz, -CH_2-), 3.34 (4H, br.s., piperazine), 4.07 (2H, br.s., piperazine), 4.28 (2H, br.s., piperazine), 4.46 (2H, s, -CH_2-), 8.34 (2H, s, -SO_2NH_2). ^{13}C NMR (75 MHz, DMSO–d_6): δ =7.88, 43.31, 45.15, 50.31, 51.16,

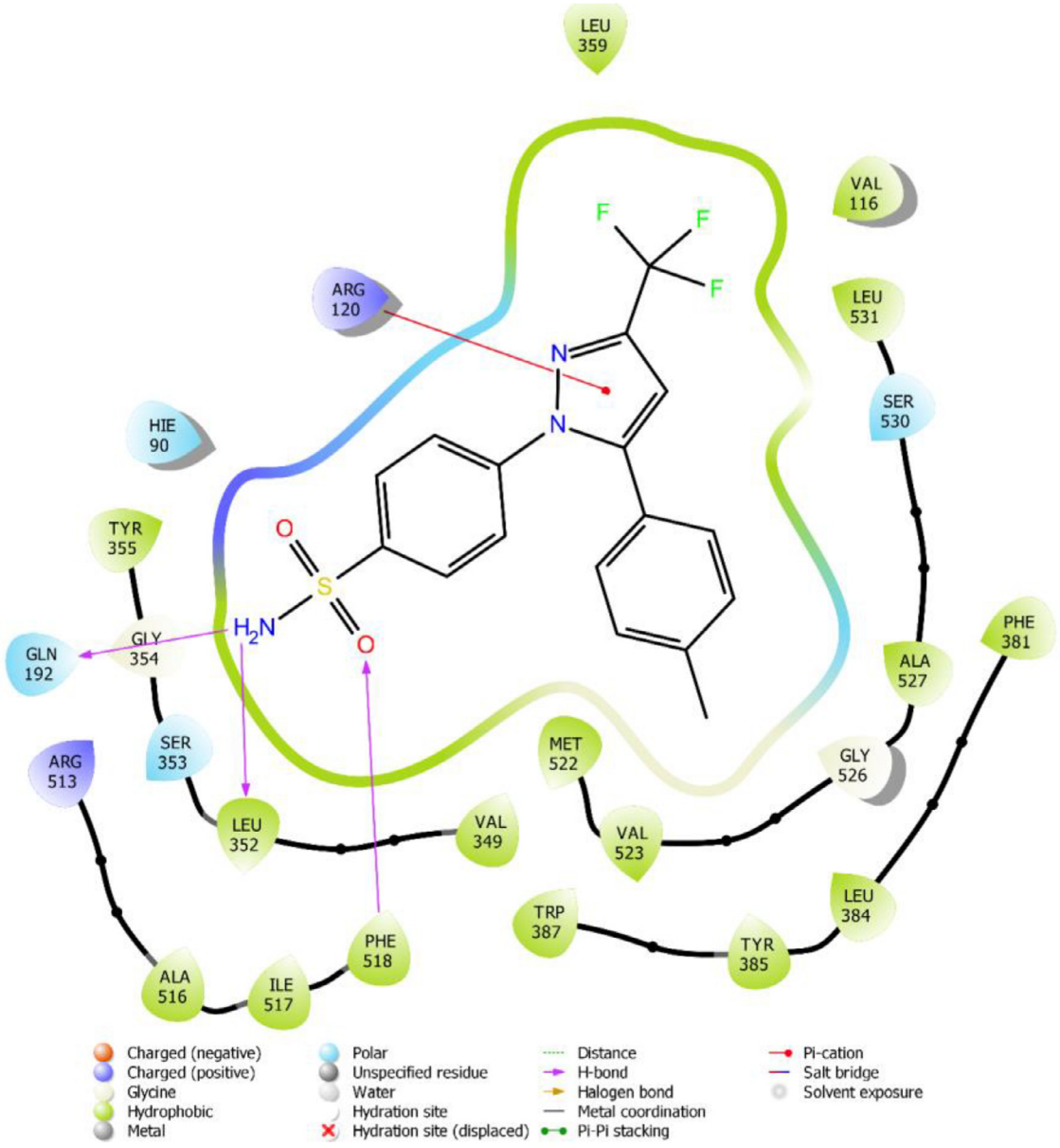

Fig. 3. The two-dimensional interacting mode of celecoxib in the active region of COX-2 (PDB ID: 6COX).

161.93, 164.78, 167.75, 195.34. HRMS (*m/z*): $[M + H]^+$ calcd for $C_{11}H_{18}N_6O_5S_5$: 475.0015; found 475.0024.

2-oxo-2-((5-sulfamoyl-1,3,4-thiadiazol-2-yl)amino)ethyl 4-cyclohexylpiperazine-1-carbodithioate (3 h)

Yield: 88%, M.P.: 230.2–231.6 °C. ^{1}H NMR (300 MHz, DMSO–d_6): δ = 1.08–1.22 (5H, m, cyclohexyl), 1.55–1.58 (1H, m, cyclohexyl), 1.72–1.75 (4H, m, cyclohexyl), 2.34 (1H, br.s., cyclohexyl), 2.62 (4H, br.s., piperazine), 3.92 (2H, br.s., piperazine), 4.16 (2H, br.s., piperazine), 4.42 (2H, s, -CH_2-), 8.31 (2H, s, -SO_2NH_2). ^{13}C NMR (75 MHz, DMSO–d_6): δ =25.65, 26.19, 28.64, 48.46, 50.75, 51.97, 62.81, 162.27, 164.59, 168.04, 194.07. HRMS (*m/z*): $[M + H]^+$ calcd for $C_{15}H_{24}N_6O_3S_4$: 465.0865; found 465.0871.

2-oxo-2-((5-(trifluoromethyl)−1,3,4-thiadiazol-2-yl)amino)ethyl pyrrolidine-1-carbodithioate (**3i**)

Yield: 83%, M.P.: 162.8–164.7 °C. ^{1}H NMR (300 MHz, DMSO–d_6): δ = 1.91–1.95 (2H, m, pyrrolidine), 2.04–2.09 (2H, m, pyrrolidine), 3.66–3.77 (4H, m, pyrrolidine), 4.46 (2H, s, -CH_2-), 13.62 (1H, s, -NH). ^{13}C NMR (75 MHz, DMSO–d_6): δ =22.45, 24.31, 26.20, 51.21, 55.79, 122.21 (q, J = 272.1 Hz), 150.96 (d, J = 37.8 Hz), 161.96, 168.08, 189.85. HRMS (*m/z*): $[M+Na]^+$ calcd for $C_{10}H_{11}N_4OF_3S_3$: 378.9939; found 378.9944.

2-oxo-2-((5-(trifluoromethyl)−1,3,4-thiadiazol-2-yl)amino)ethyl piperidine-1-carbodithioate (**3j**)

Yield: 78%, M.P.: 170.8–172.9 °C. ^{1}H NMR (300 MHz, DMSO–d_6): δ = 1.59–1.64 (6H, m, piperidine), 3.93 (2H, br.s., piperidine), 4.18 (2H, br.s., piperidine), 4.46 (2H, s, -CH_2-), 13.64 (1H, s, -NH). ^{13}C NMR (75 MHz, DMSO–d_6): δ =23.86, 25.61, 26.32, 40.07, 41.94, 51.73, 53.13, 120.41 (J = 271.7 Hz), 150.94 (J = 37.6 Hz), 161.97, 168.13, 192.73. HRMS (*m/z*): $[M+Na]^+$ calcd for $C_{11}H_{13}N_4OF_3S_4$: 393.0096; found 393.0108.

2-oxo-2-((5-(trifluoromethyl)−1,3,4-thiadiazol-2-yl)amino)ethyl 4-methylpiperidine-1-carbodithioate (**3k**)

Yield: 77%, M.P.: 122.8–124.8 °C. ^{1}H NMR (300 MHz, DMSO–d_6): δ = 0.93 (3H, d, J = 6.3 Hz, -CH_3), 1.12–1.19 (2H, m, piperidine), 1.72–1.82 (3H, m, piperidine), 3.16–3.24 (1H, m, piperidine), 3.36–3.45 (1H, m, piperidine), 4.46 (3H, br.s., -CH_2-, piperidine), 5.14–5.19 (1H, m, piperidine), 13.64 (1H, s, -NH). ^{13}C NMR (75 MHz, DMSO–d_6): δ = 21.50, 30.35, 33.61, 34.23, 43.01, 50.84, 52.35,

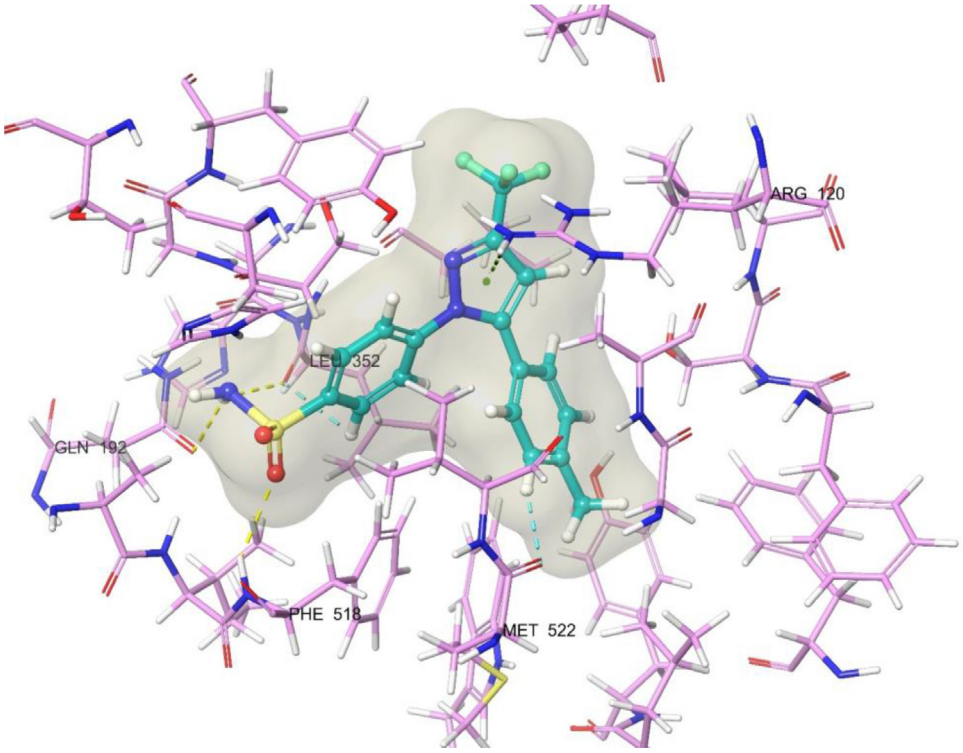

Fig. 4. The 3D interacting mode of celecoxib in the active region of COX-2 enzyme (PDB Code: 6COX). Celecoxib is shown in a tube pattern and turquoise colored.

120.42 (J = 271.9 Hz), 150.65 (J = 37.6 Hz), 162.01, 168.15, 192.86. HRMS (m/z): $[M+Na]^+$ calcd for $C_{12}H_{15}N_4OF_3S_3$: 407.0252; found 407.0268.

*2-oxo-2-((5-(trifluoromethyl)−1,3,4-thiadiazol-2-yl)amino)ethyl 4-methylpiperazine-1-carbodithioate (**3l**)*

Yield: 85%, M.P.: 153.6–154.7 °C. ^{1}H NMR (300 MHz, DMSO–d_6): δ = 2.34 (3H, s, -CH_3), 2.61 (4H, br.s., piperazine), 4.01 (2H, br.s., piperazine), 4.22 (2H, br.s., piperazine), 4.46 (2H, s, -CH_2), 12.95 (1H, s, -NH). ^{13}C NMR (75 MHz, DMSO–d_6): δ = 42.25, 45.49, 47.32, 51.82, 53.69, 55.53, 120.48 (J = 271.9 Hz), 150.47 (J = 37.3 Hz), 162.43, 168.19, 194.86. HRMS (m/z): $[M + H]^+$ calcd for $C_{11}H_{14}N_5OF_3S_3$: 386.0385; found 386.0377.

*2-oxo-2-((5-(trifluoromethyl)−1,3,4-thiadiazol-2-yl)amino)ethyl 4-ethylpiperazine-1-carbodithioate (*3 m*)*

Yield: 83%, M.P.: 182.5–184.5 °C. ^{1}H NMR (300 MHz, DMSO–d_6): δ = 1.05 (3H, t, J = 7.2 Hz, -CH_3), 2.46–2.51 (2H, m, -CH_2-), 2.60 (4H, br.s., piperazine), 3.99 (2H, br.s., piperazine), 4.21 (2H, br.s., piperazine), 4.45 (2H, s, -CH_2-). ^{13}C NMR (75 MHz, DMSO–d_6): δ = 11.96, 49.88, 51.06, 51.41, 51.87, 120.53 (J = 271.9 Hz), 150.53 (J = 37.4 Hz), 162.78, 168.42, 194.47. HRMS (m/z): $[M + H]^+$ calcd for $C_{12}H_{16}N_5OF_3S_3$: 400.0542; found 400.0533.

*2-oxo-2-((5-(trifluoromethyl)−1,3,4-thiadiazol-2-yl)amino)ethyl 4-(methylsulfonyl)piperazine-1-carbodithioate (**3n**)*

Yield: 80%, M.P.: 216.3–217.9 °C. ^{1}H NMR (300 MHz, DMSO–d_6): δ = 2.94 (3H, s, -CH_3), 3.28 (4H, br.s., piperazine), 4.10 (2H, br.s., piperazine), 4.32 (2H, br.s., piperazine), 4.50 (2H, s, -CH_2), 13.66 (1H, s, -NH). ^{13}C NMR (75 MHz, DMSO–d_6): δ = 33.88, 35.72, 42.04, 43.47, 45.37, 47.18, 120.41 (J = 272.0 Hz), 150.95 (J = 37.5 Hz), 162.04, 167.92, 195.19. HRMS (m/z): $[M+Na]^+$ calcd for $C_{11}H_{14}N_5O_3F_3S_4$: 471.9824; found 471.9835.

*2-oxo-2-((5-(trifluoromethyl)−1,3,4-thiadiazol-2-yl)amino)ethyl 4-(ethylsulfonyl)piperazine-1-carbodithioate (**3o**)*

Yield: 81%, M.P.: 180.2–181.8 °C. ^{1}H NMR (300 MHz, DMSO–d_6): δ = 1.22 (3H, t, J = 7.4 Hz, -CH3), 3.11 (2H, q, J = 7.3 Hz, -CH_2-), 3.34 (4H, br.s., piperazine), 4.06 (2H, br.s., piperazine), 4.28 (2H, br.s., piperazine), 4.49 (2H, s, -CH_2-), 13.06 (1H, s, -NH). ^{13}C NMR (75 MHz, DMSO–d_6): δ = 7.87, 40.10, 43.25, 45.15, 50.28, 51.23, 120.40 (J = 271.9 Hz), 150.99 (J = 37.5 Hz), 161.95, 167.89, 195.18. HRMS (m/z): $[M + H]^+$ calcd for $C_{12}H_{16}N_5O_3F_3S_4$: 464.0161; found 464.0159.

*2-oxo-2-((5-(trifluoromethyl)−1,3,4-thiadiazol-2-yl)amino)ethyl 4-cyclohexylpiperazine-1-carbodithioate (**3p**)*

Yield: 83%, M.P.: 168.5–170.1 °C. ^{1}H NMR (300 MHz, DMSO–d_6): δ = 1.16–1.19 (5H, m, -cyclohexyl), 1.54–1.58 (1H, m, -cyclohexyl), 1.73–1.78 (4H, m, -cyclohexyl), 2.42 (1H, br.s., -cyclohexyl), 2.69 (4H, m, piperazine), 3.95 (2H, br.s., piperazine), 4.19 (2H, br.s., piperazine), 4.44 (2H, s, -CH_2-). ^{13}C NMR (75 MHz, DMSO–d_6): δ = 25.56, 26.08, 28.46, 48.40, 50.38, 51.59, 62.97, 120.53 (J = 271.9 Hz), 150.51 (J = 37.4 Hz), 162.77, 168.43, 194.23. HRMS (m/z): $[M + H]^+$ calcd for $C_{16}H_{22}N_5OF_3S_3$: 454.1011; found 454.0992.

2.2. In vitro *COX-1 and COX-2 inhibition assay*

The *in vitro* inhibitory potency of the compounds against COX-1/COX-2 was measured by using fluorometric COX-1 and COX-2 inhibitor screening kits (Biovision, Switzerland) according to the manufacturer's instructions [24,25]. The assay is based on the fluorometric detection of prostaglandin G_2, the intermediate product generated by the COX enzyme. The *in vitro* COX inhibition test was performed using the available fluorometric method, and the percentages and IC_{50} values of obtained compounds were calculated as previously described by our research group [15,26].

2.3. *Molecular docking studies*

Molecular docking studies were carried out using a structure-based protocol to reveal the binding mechanisms of compound **3d** to the active site of the COX-2 enzyme. For this purpose, the crystal structure of COX-2 crystallized with celecoxib (PDB ID: 6COX) [27] was extracted from the Protein Data Bank database (www.pdb.org).

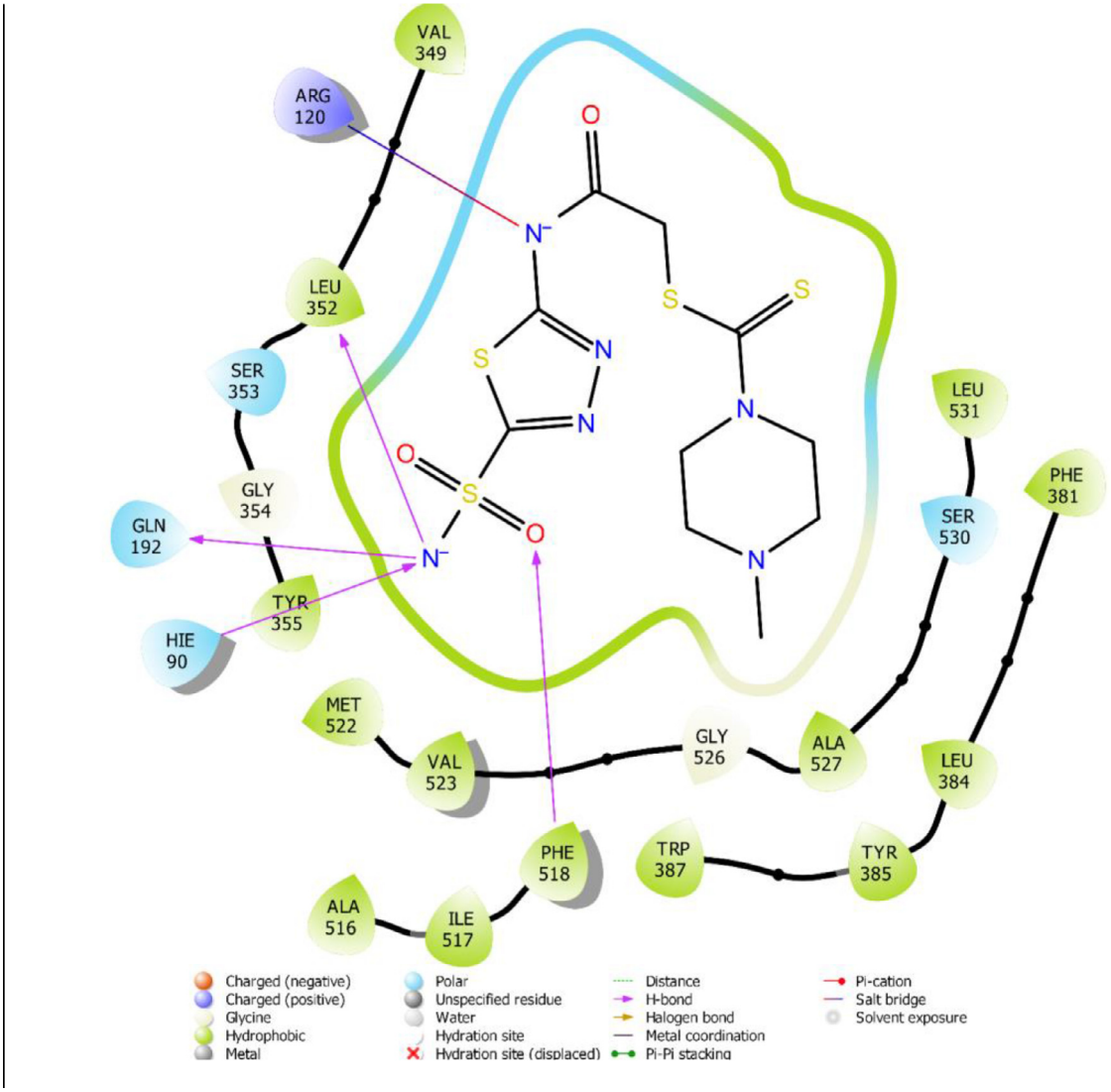

Fig. 5. The two-dimensional interacting mode of compound 3d in the active region of COX-2 (PDB ID: 6COX).

The ligands' configurations were designed using the *Schrödinger Maestro* [28] tool and submitted to the *Schrödinger Suite 2020 Update 2 Protein Preparation Wizard* method. The ligands were processed using *LigPrep 3.8* [29] to correctly detect the atom groups as well as the protonation conditions at a pH of 7.4 ± 1.0. Bond orders were assigned, and hydrogen atoms were added to the structures. *Glide 7.1* was used to construct the grid generation [30]. Flexible ligand docking runs were performed in standard-precision docking mode (SP).

2.4. Molecular dynamic simulations

Molecular dynamic (MD) simulations are considered an important computational tool for evaluating the time-dependent stability of a ligand in an active site for a drug–receptor complex [31]. MD simulations for 50 ns were carried out to ensure the stability of the identified hits from the docking result. We performed the Desmond application [32] using the standard force field (OPLS3e) of the Schrodinger Suite with a transferable intermolecular potential with a 3 points (TIP3P) water model followed by energy minimization of the complex [33]. The neutralization of the system was achieved using Na^+ and Cl^- ions to provide a final salt concentration of 0.15 M in order to simulate physiological concentration of monovalent ions [34]. Constant temperature (300 K) and pressure (1.01325 bar) were employed with NPT (constant number of particles, pressure, and temperature) as ensemble class. RESPA integrator [35] was used in order to integrate the equations of motion. NH thermostats [36] were used to keep the constant simulation temperature, and the MTK method [37] was applied to control the pressure. Long-range electrostatic interactions were calculated by pmE method [38]. The cutoff for van der Waals and short-range electrostatic interactions was set at 9.0 Å. The equilibration of the system was performed with the default protocol provided in Desmond, which consists of a series of restrained minimizations and molecular dynamics simulations used to slowly relax the system. This procedure was also previously applied by our *in silico* study group [39]. The MD simulation was performed using above settings and following the completion of the system setup. Rg (radius of gyration), root mean square fluctuation (RMSF) and root mean square deviation (RMSD) values were calculated by the Desmond application [32].

3. Result and discussion

3.1. Chemistry

The compounds **3a**-**3l** were synthesized as presented in Scheme 1. Initially, compound **1a** and **1b** were produced by means

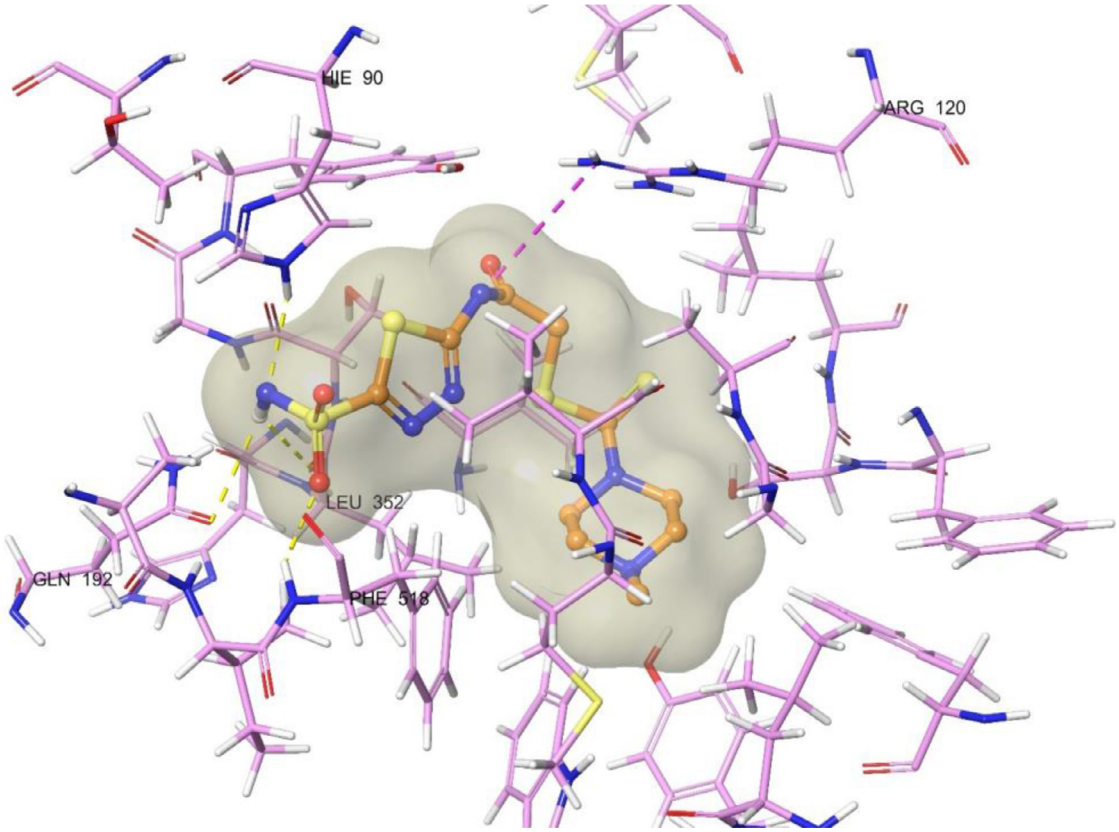

Fig. 6. The 3D interacting mode of compound 3d in the active region of COX-2 enzyme (PDB Code: 6COX). Compound 3d is shown in a tube pattern and orange colored.

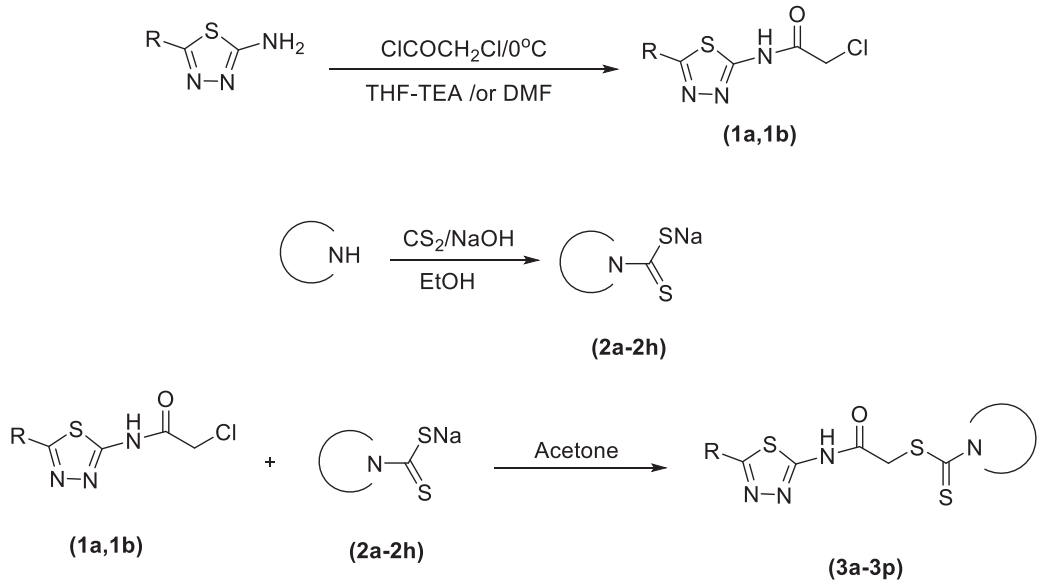

Scheme 1. Synthesis pathway for obtained compounds (**3a-3p**).

of the acetylation reaction. No product was obtained when THF was used to obtain compound **1a**. Therefore, the reaction solvent was changed to DMF. Unlike the standard acetylation procedure, it was carried out in DMF without using a catalyst. Compounds **2a-**2 h were obtained by the reaction of appropriate secondary amine and carbon disulfide in the presence of NaOH. Compounds **1a-1b** and compound **2a-**2 h were reacted in acetone to yield the final products. The structures of the compounds obtained were verified using spectroscopic methods, namely ^{1}H NMR, ^{13}C NMR, and HRMS (**Supplementary Data**).

When the ^{1}H NMR data of the compounds were examined, it was observed that the pyrrolidine-containing compounds (**3a** and **3i**) gave peaks between 1.90 ppm and 3.77 ppm. The protons of piperidine of compounds containing piperidine (**3b, 3c, 3j** and **3k**) were observed between 1.12 ppm and 5.19 ppm. Protons of the piperazine ring were detected between 2.47 ppm and 4.32 ppm (**3d-**3 h, **3l-3p**). Methylene group protons were distinguished as singlet between 4.42 ppm and 4.50 ppm values. Protons of the sulfonamide structure (**3a**-3 h) were determined as singlet between 8.29 ppm and 8.36 ppm values. Protons belonging to the

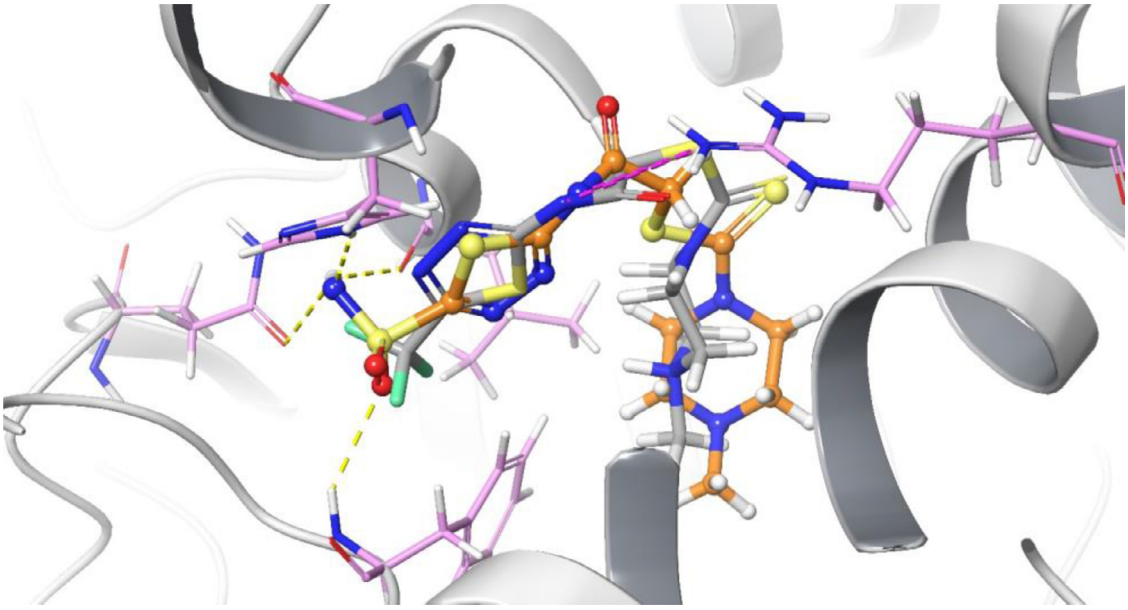

Fig. 7. The superimposition poses of compound 3d and compound 3l in the enzyme active site (PDB Code: 6COX). Compound 3d and 3l is shown in a tube pattern and orange, gray colored respectively.

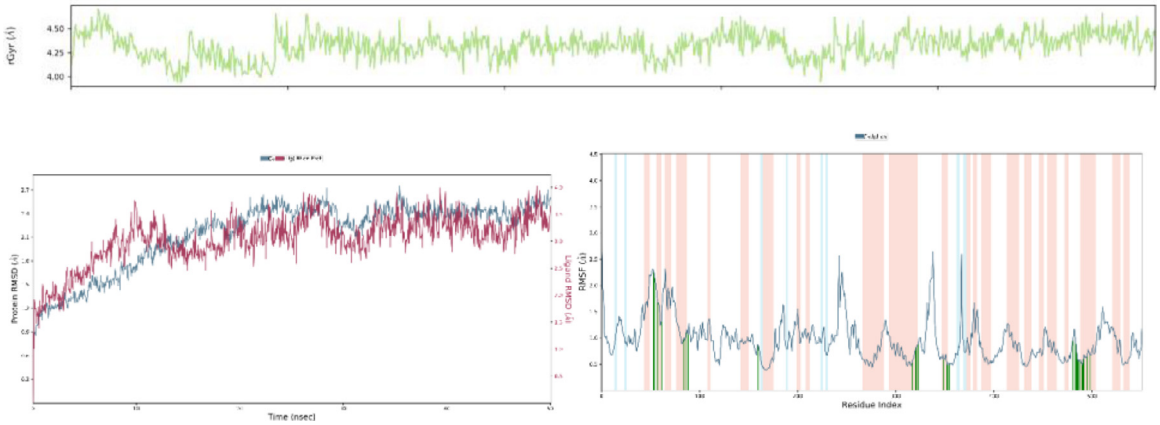

Fig. 8. Stability diagrams of compound 3d-COX-2 enzyme complex. Top: Plot of radius of gyration-time (ns), Left side: Plot of RMSD (Å)-time (ns), Right side: Plot of RMSF-residue index (The areas were represented in light red for the helices, light blue for the strands, and white for the loops).

amide group were recognized as singlet between 12.95 ppm and 13.66 ppm values.

When the ^{13}C NMR data of the compounds were analyzed, the protons belonging to the carbonyl (C = O) group were observed between 167.75 ppm and 168.43 ppm values. The peak of C = S group was detected between 189.94 ppm and 195.44 ppm values. The peaks of the CF_3 group (**3i-3p**) were shown between 120.53 ppm and 122.21 ppm values with J = 271.7–272.1 Hz. The thiadiazol carbon, to which the CF_3 group is attached, was detected between 150.51 ppm and 150.99 ppm values with J = 37.3–37.8 Hz.

3.2. COX inhibition assay

All obtained thiadiazol derivatives were evaluated for their ability to inhibit COX-1 and COX-2 enzymes using fluorometric inhibitor screening kits (Biovision, Switzerland). Evaluation criteria were performed according to the manufacturer's instructions [24,25]. According to the inhibition percentages and concentrations of the compounds, enzyme activity experiments were carried out in 2 stages. Synthesized compounds and reference agents prepared at 10^{-3} and 10^{-4} M concentrations were used for the first step of the assay. The results of this step are given in Table 1. Compounds with more than 50% inhibitory activity at the concentration of 10^{-4} M were preferred for step 2. The selected compounds and reference agents were prepared in their further concentrations by serial dilutions (ranging from 10^{-5} M to 10^{-9} M) for second step. At the end of the second step, the half-maximum inhibitory concentration (IC_{50}) values of the selected compounds and reference inhibitors were calculated, and these results are given in Tables S1 and **2**.

Most of the tested compounds showed greater than 50% inhibitory activity for both COX-1 and COX-2 enzymes at 10^{-3} M concentration (as seen in Table 1). Similar efficacy was not observed for inhibition at 10^{-4} M concentration . None of the compounds showed significant activity against the COX-1 enzyme at a concentration of 10^{-4} M. On the other hand, compounds **3c** and **3d** demonstrated more than 50% inhibitory activity on COX-2 enzyme. Therefore, compounds **3c** and **3d** were chosen for the second step of the inhibition analysis to determine their IC_{50} values as shown in Table 2. Generally, it could be concluded that all synthesized compounds showed selective inhibitory potency against COX-2 enzyme. Among the selected derivatives, compound **3d** was found to be the most active agent with an IC_{50} value of 0.134±0.004 μM.

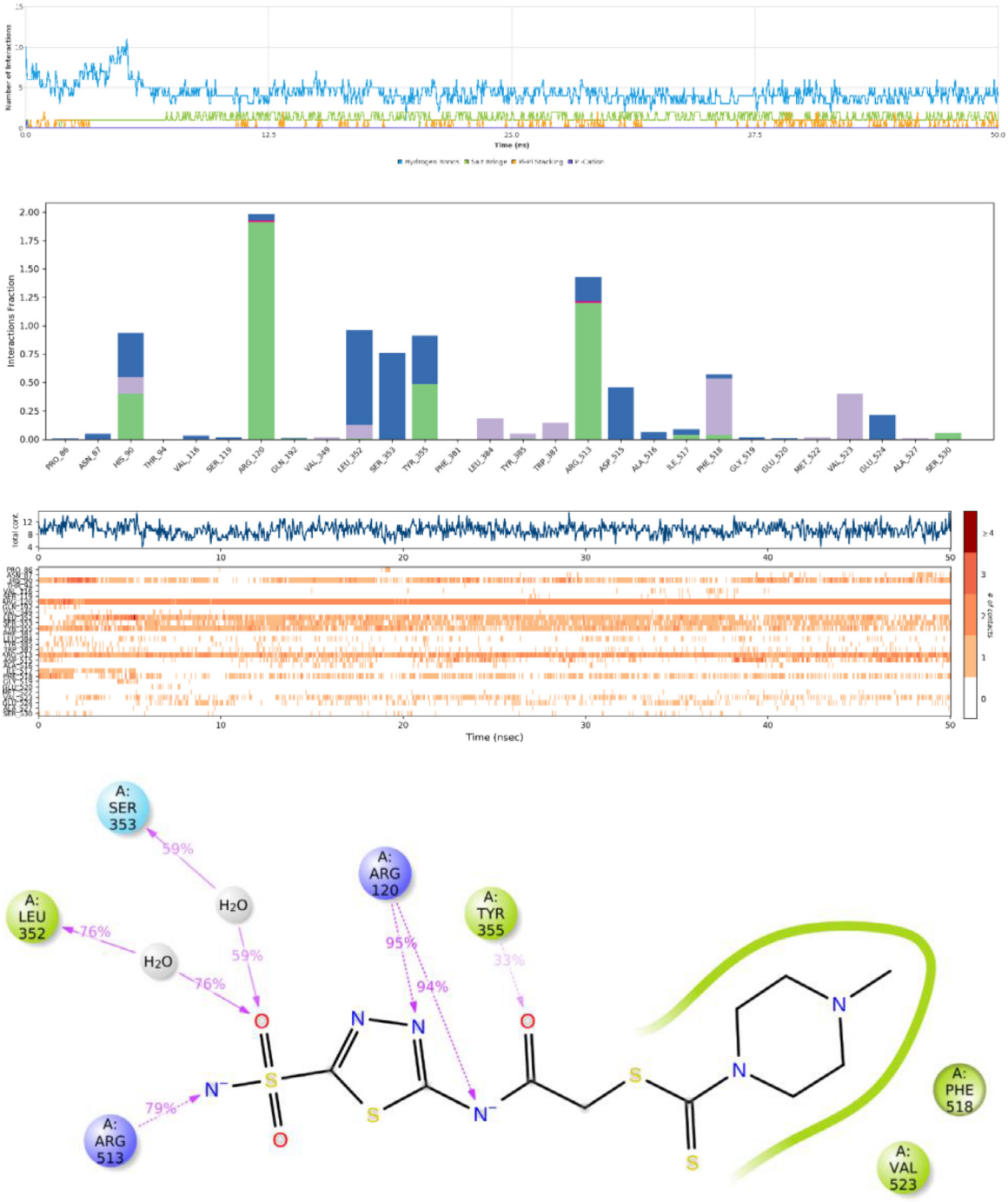

Fig. 9. Interactions diagrams of compound 3d-COX-2 enzyme complex. First: The plot of number of interactions and their types; Second: Interaction fractions by residue during the simulation (Blue: water mediated H-bond; green: H-bond, pink: ionic interaction, purple: hydrophobic interaction); Third: Plot of number of interactions-residue index; Fourth: Diagram of the interaction strengths (cut off 30%).

When this value compared to that of reference drugs, it was seen that compound **3d** displayed a similarly inhibition profile with celecoxib (IC_{50}=0.132±0.005 μM).

When the activity results were examined, it was recognized that the derivatives containing sulfonamide (**3a**-3 h) were more active than the derivatives containing CF_3 (**3i**-**3p**). Among the derivatives containing sulfonamide substituent, compounds **3c** and **3d** exhibited higher activity comparing to the other compounds. Compound **3c** possesses a 4-methylpiperidine ring, while compound **3d** has a 4-methylpiperazine ring. It was also revealed that compounds containing a 6-membered ring in their skeleton were more active than compounds having 5-membered ring (**3a**). In addition, the methyl substituent placed at the 4th position among the 6-membered rings contributed significantly to the activity. It was observed that the activity decreased as the substituent at this position grows. Moreover, the introduction of methyl sulfonyl, ethyl sulfonyl or cyclohexyl bulky groups in this position resulted in reduced activity compared to the 5-membered ring containing derivatives

3.3. Molecular docking

As mentioned in the COX enzymes inhibitory activity assay, compound **3d** was found to be the most active derivative in the se-

Table 1
% Inhibition of the synthesized compounds, ibuprofen, celecoxib and nimesulide against COX-1 and COX-2 enzymes.

Compounds	COX-1% Inhibition		COX-2% Inhibition	
	10^{-3} M	10^{-4} M	10^{-3} M	10^{-4} M
3a	50.2 ± 0.9	38.4 ± 1.2	80.5 ± 2.0	48.9 ± 1.3
3b	53.4 ± 1.7	41.5 ± 0.9	85.3 ± 2.0	48.4 ± 1.6
3c	59.4 ± 1.6	46.2 ± 1.1	**89.6 ± 0.3**	**77.6 ± 0.8**
3d	65.6 ± 1.3	48.4 ± 0.9	**93.2 ± 0.1**	**87.9 ± 0.1**
3e	60.2 ± 0.9	41.4 ± 1.4	80.5 ± 1.5	51.3 ± 1.5
3f	51.3 ± 1.7	38.3 ± 1.1	66.3 ± 2.1	48.1 ± 1.0
3 g	48.9 ± 1.4	34.2 ± 1.0	59.1 ± 1.1	42.4 ± 2.1
3h	49.5 ± 1.9	36.3 ± 1.0	61.3 ± 1.9	43.5 ± 1.0
3i	45.3 ± 2.0	31.1 ± 0.9	65.0 ± 2.1	42.3 ± 1.6
3j	47.5 ± 1.6	33.9 ± 0.9	70.5 ± 1.5	45.4 ± 1.6
3k	52.2 ± 1.0	38.4 ± 1.3	75.3 ± 1.6	49.0 ± 1.0
3l	58.4 ± 0.9	35.4 ± 0.8	78.4 ± 1.1	50.6 ± 1.5
3m	49.1 ± 1.6	30.5 ± 1.3	69.6 ± 1.0	44.2 ± 1.3
3n	44.1 ± 1.2	27.3 ± 1.0	58.7 ± 2.0	40.3 ± 1.9
3o	40.4 ± 1.2	21.3 ± 0.9	55.9 ± 1.9	37.5 ± 2.0
3p	42.2 ± 1.9	25.2 ± 0.7	59.2 ± 1.7	35.1 ± 1.9
Ibuprofen	98.2 ± 1.1	89.4 ± 1.2	98.2 ± 1.2	88.2 ± 1.3
Celecoxib	–	–	92.3 ± 1.4	85.5 ± 1.3
Nimesulide	–	–	97.8 ± 1.2	89.6 ± 1.0

Table 2
IC_{50} values of 3c, 3d, ibuprofen, celecoxib and nimesulide against COX-2.

Compounds	IC_{50} (μM)
3c	0.350±0.015
3d	0.134±0.004
Ibuprofen	5.326±0.218
Celecoxib	0.132±0.005
Nimesulide	1.684±0.079

ries against COX-2 enzyme. After determination of the most potent compound, we performed the docking study. By applying molecular docking studies, further information about the binding mode of compound **3d** and the impact of structural modifications on the inhibitory activity against COX-2 enzyme have been evaluated. Studies were performed using the X-ray crystal structure of COX-2 (COX-2 PDB Code: 6COX) [27] retrieved from Protein Data Bank database (www.pdb.org). Firstly, the docking procedure was validated by executing the protocol with celecoxib. Validated docking pose are presented in the supplementary file in overlapping form (Fig. S1). Then, compound **3d** was subjected to the same docking procedure. The rendered docking poses of celecoxib and compound **3d** are presented in Figs. 2-**6**. Fig. 2 shows the positions of active compound **3d** and celecoxib into the enzyme active site. Compound **3d** were fitted into the enzyme active site similarly to celecoxib.

The results showed that there were three hydrogen bond and single π-cation bond between celecoxib and COX-2. The amino group of sulfonamides established two hydrogen bonds with carbonyls of Gln192 and carbonyls of Leu352. The oxygen atoms of sulfonamide formed one hydrogen bond with the Phe518 amino group. There was also a single π-cation interaction between the pyrazole ring of the celecoxib and amino groups of Arg120 (Figs. 3 and **4**).

The results showed that there were four hydrogen bond and one salt bride bond between compound **3d** and COX-2. The amino group of sulfonamides established three hydrogen bonds with the carbonyls of Gln192, the carbonyls of Leu352 and hydrogens of imidazole's of Hie90. The oxygen atoms of sulfonamide established one hydrogen bond with amino group of Phe518. There was also a π-cation interaction between the amide group of the compound **3d** and amino groups of Arg120 (Figs. 5 and 6).

Subsequently, consistent results were obtained when compared with the activity results. The derivative that have a six-membered ring with methyl substitution was the most active derivative and interacted with the enzyme active site in a similar way to celecoxib. The docking pose for compound **3f** were further analyzed to investigate at the positioning in the enzyme active site when a bulkier substituent replaced the methyl group. Relevant docking poses are presented in the supplementary file. Examining Figs. S2 and **S3**, it was observed that the compound was not fully fitted into the enzyme active site.

Derivatives containing sulfonamides (**3a-**3 h) appear to be more effective in general. This difference in activity between CF_3-containing derivatives and sulfonamide-containing derivatives may be due to the good positioning of the sulfonamide group in the hydrophobic pocket of the COX-2 enzyme and its interactions there. In Fig. 7, the overlapping poses of compound **3d** and compound **3l** in the active site is presented. Both compounds contain methyl piperazine. The distinguished difference in their structure is that one carries sulfonamide and the other CF_3. When the figure was examined, it was observed that the sulfonamide structure is fully placed in this pocket (Fig. 7).

3.4. Molecular dynamic simulation (MDS) studies

The stability was checked by following rules: 1. RMSD value of protein was calculated between 1 and 3 Å during the entire simulation, which is indicative of stability for small proteins [32]; 2. In Rg and RMSF plots, picks should have minimum fluctuation; 3. The loop (white area) region may show big fluctuation. In this simulation, the stability properties displayed that the system was not stable until 10 ns (the equilibration phase), and after that, the system stability was reached. Also, one of the loop regions was detected with minimal fluctuation (Fig. 8).

According to Fig. 9, the interaction with the Arg120 amino acid is key point for the activity. During the entire simulation, the interaction with this residue never cut off, and it had very strong contact power, which enabled the protection of the stability. Arg120 has interacted with thiadiazol N_4 and acetamide nitrogen via H-bonds. As previously mentioned in the introduction section, the relation between the COX inhibition and this amino acid was clarified, in our study, we also observed that. Besides, Arg513 was also another non-stop interacted amino acid which interacted with sulphonyl amide nitrogen. Also, until 10 ns, there were several interactions between ligand and His90, but after that time, although the interactions were occasionally seen until the end of the simulation, they were not continually. On the contrary to His90, the frequency of the interaction with Ser353 was increasing after 10 ns. The interactions with Leu352 and Tyr355 observed with high frequency during the entire simulation. All these residues could have a significant impact on stability. Moreover, the simulation can be split into two parts, and the 10 ns could be marked as a milestone for the stability and so for the activity. Besides, His90 amino acid was described as one of the important residues for COX-2 selectivity, we found that it was breaking the stability on contrary to the description in this study. Furthermore, Arg513 residue was identified as another crucial residue to evaluate COX-2 activity and selectivity, which was found to be consistent with the literature [40, 41]. Moreover, it was proposed that the COX-2 selectivity of compound **3d** was especially related to interaction strength and type with Arg513. Additionally, aromatic H-bonds were detected between sulphonamide oxygens and His90, Tyr355, and Phe518; acetamide oxygen and Tyr355. Although the aromatic H-bond with His90 was incrementally established over the course of the simulation and broke after 10 nanoseconds, similarly to the H-bond interaction, it could strengthen the COX-2 inhibition.

Another important result was about the water molecules which played an important role to protect the complex stability and therefore the inhibition activity. Water-mediated H-bonds were seen with Asn87, His90, Val116, Ser119, Arg120, Gln192, Leu352, Ser353, Tyr355, Asp515, Phe518, Gly519, Glu520, and Glu524. Especially, when the water-mediated H-bonds with Leu352 and Ser353 were in contact with the ligand, the selective COX-2 inhibition activity has been increasing because these residues were blocked in COX-1. Hence, the sulfonamide group was determined as an important pharmacophore moiety to display selective COX-2 activity.

In summary, this study established that COX-2 activity was mediated by H-bonds with Arg120 and Tyr355, while COX-2 selectivity was mediated by H-bonds with Arg513, Leu352, and Ser353.

4. Conclusion

In this study, 16 new thiadiazole derivatives were synthesized. One half of these compounds carry sulfonamide group while the other half have CF_3 substitution. Derivatives containing sulfonamides exhibited superior activity and selectivity towards COX-2 enzyme. It was also observed that the methyl substitution attached to the 4th position of the piperazine ring increased the activity. As this substitution grows, the activity decreases. When the piperazine ring is replaced by the piperidine ring, the activity decreases. Molecular docking studies have shown that compound **3d** is localized at the same enzyme active site as celecoxib and gives the same interactions. Molecular dynamics studies are also compatible with activity studies. However, the loss of continuity of interactions between ligand and His90 after 10 ns is thought to be due to the positioning of the sulfonamide group. The sulfonamide group might be located closer to the His90 amino acid if it was attached to a larger ring. To investigate this effect, it is proposed to insert larger rings instead of the thiadiazole in future studies.

Declaration of Competing Interest

The authors declare that they have no known competing financial interests or personal relationships that could have appeared to influence the work reported in this paper.

CRediT authorship contribution statement

Derya Osmaniye: Visualization, Writing – original draft, Writing – review & editing, Investigation, Formal analysis, Software, Methodology, Conceptualization. **Asaf Evrim Evren:** Writing – original draft, Writing – review & editing, Software, Methodology. **Şevval Karaca:** Methodology. **Yusuf Özkay:** Supervision, Visualization, Investigation, Conceptualization. **Zafer Asım Kaplancıklı:** Investigation, Conceptualization, Supervision.

Data Availability

Data will be made available on request.

Acknowledgments

As the authors of this study, we thank Anadolu University Faculty of Pharmacy Central Analysis Laboratory for their support and contributions.

Supplementary materials

Supplementary material associated with this article can be found, in the online version, at doi:10.1016/j.molstruc.2022.134171.

References

[1] M.A. Meshram, U.O. Bhise, P.N. Makhal, V.R. Kaki, Synthetically-tailored and nature-derived dual COX-2/5-LOX inhibitors: structural aspects and SAR, Eur. J. Med. Chem. (2021) 113804.
[2] T. Güngör, A. Özleyen, Y.B. Yılmaz, P. Siyah, M. Ay, S. Durdağı, T.B. Tumer, New nimesulide derivatives with amide/sulfonamide moieties: selective COX-2 inhibition and antitumor effects, Eur. J. Med. Chem. (2021) 113566.
[3] P.A. Halim, H.H. Georgey, M.Y. George, A.M. El Kerdawy, M.F. Said, Design and synthesis of novel 4-fluorobenzamide-based derivatives as promising anti-inflammatory and analgesic agents with an enhanced gastric tolerability and COX-inhibitory activity, Bioorg. Chem. 115 (2021) 105253.
[4] M.F. Said, H.H. Georgey, E.R. Mohammed, Synthesis and computational studies of novel fused pyrimidinones as a promising scaffold with analgesic, anti-inflammatory and COX inhibitory potential, Eur. J. Med. Chem. 224 (2021) 113682.
[5] H. Yao, Q. Guo, M. Wang, R. Wang, Z. Xu, Discovery of pyrazole N-aryl sulfonate: a novel and highly potent cyclooxygenase-2 (COX-2) selective inhibitors, Bioorg. Med. Chem. 46 (2021) 116344.
[6] A.R. Nesaragi, R.R. Kamble, S. Dixit, B. Kodasi, S.R. Hoolageri, P.K. Bayannavar, J.P. Dasappa, S. Vootla, S.D. Joshi, V.M. Kumbar, Green synthesis of therapeutically active 1, 3, 4-oxadiazoles as antioxidants, selective COX-2 inhibitors and their in silico studies, Bioorg. Med. Chem. Lett. 43 (2021) 128112.
[7] A.A. Marzouk, E.S. Taher, M.S.A. Shaykoon, P. Lan, W.H. Abd-Allah, A.M. Aboregela, M.F. El-Behairy, Design, synthesis, biological evaluation, and computational studies of novel thiazolo-pyrazole hybrids as promising selective COX-2 inhibitors: implementation of apoptotic genes expression for ulcerogenic liability assessment, Bioorg. Chem. 111 (2021) 104883.
[8] A.M. Alfayomy, S.A. Abdel-Aziz, A.A. Marzouk, M.S.A. Shaykoon, A. Narumi, H. Konno, S.M. Abou-Seri, F.A. Ragab, Design and synthesis of pyrimidine-5-carbonitrile hybrids as COX-2 inhibitors: anti-inflammatory activity, ulcerogenic liability, histopathological and docking studies, Bioorg. Chem. 108 (2021) 104555.
[9] Y. El-Dash, N.A. Khalil, E.M. Ahmed, M.S. Hassan, Synthesis and biological evaluation of new nicotinate derivatives as potential anti-inflammatory agents targeting COX-2 enzyme, Bioorg. Chem. 107 (2021) 104610.
[10] K.R. Abdellatif, E.K. Abdelall, M.B. Labib, W.A. Fadaly, T.H. Zidan, Synthesis of novel halogenated triarylpyrazoles as selective COX-2 inhibitors: anti-inflammatory activity, histopatholgical profile and in-silico studies, Bioorg. Chem. 105 (2020) 104418.
[11] N.H. Metwally, M.S. Mohamed, New imidazolone derivatives comprising a benzoate or sulfonamide moiety as anti-inflammatory and antibacterial inhibitors: design, synthesis, selective COX-2, DHFR and molecular-modeling study, Bioorg. Chem. 99 (2020) 103438.
[12] M.J. Lucido, B.J. Orlando, A.J. Vecchio, M.G. Malkowski, Crystal structure of aspirin-acetylated human cyclooxygenase-2: insight into the formation of products with reversed stereochemistry, Biochemistry 55 (2016) 1226–1238.
[13] M.T.-E. Maghraby, O.M. Abou-Ghadir, S.G. Abdel-Moty, A.Y. Ali, O.I. Salem, Novel class of benzimidazole-thiazole hybrids: the privileged scaffolds of potent anti-inflammatory activity with dual inhibition of cyclooxygenase and 15-lipoxygenase enzymes, Bioorg. Med. Chem. 28 (2020) 115403.
[14] R. Pouplana, J. Lozano, J. Ruiz, Molecular modelling of the differential interaction between several non-steroidal anti-inflammatory drugs and human prostaglandin endoperoxide H synthase-2 (h-PGHS-2), J. Molecul. Graph. Model. 20 (2002) 329–343.
[15] B.N. Sağlık, D. Osmaniye, S. Levent, U.A. Çevik, B.K. Çavuşoğlu, Y. Özkay, Z.A. Kaplancıklı, Design, synthesis and biological assessment of new selective COX-2 inhibitors including methyl sulfonyl moiety, Eur. J. Med. Chem. 209 (2021) 112918.
[16] E.M. Gedawy, A.E. Kassab, A.M. El Kerdawy, Design, synthesis and biological evaluation of novel pyrazole sulfonamide derivatives as dual COX-2/5-LOX inhibitors, Eur. J. Med. Chem. 189 (2020) 112066.
[17] E.S. Taher, T.S. Ibrahim, M. Fares, A.M. Al-Mahmoudy, A.F. Radwan, K.Y. Orabi, O.I. El-Sabbagh, Novel benzenesulfonamide and 1, 2-benzisothiazol-3 (2H)-one-1, 1-dioxide derivatives as potential selective COX-2 inhibitors, Eur. J. Med. Chem. 171 (2019) 372–382.
[18] H.A. Abdel-Aziz, K.A. Al-Rashood, K.E.H. ElTahir, G.M. Suddek, Synthesis of N-benzenesulfonamide-1H-pyrazoles bearing arylsulfonyl moiety: novel celecoxib analogs as potent anti-inflammatory agents, Eur. J. Med. Chem. 80 (2014) 416–422.
[19] D. Priya, M. Kathiravan, Molecular insights into benzene sulphonamide substituted diarylpyrazoles as cyclooxygenase-2 inhibitor and its structural modifications, J. Biomolecul. Struct. Dyn. (2020) 1–12.
[20] T.S. Ibrahim, I.M. Salem, S.M. Mostafa, O.I. El-Sabbagh, M.K. ElKhamisi, L. Hegazy, B. Elgendy, Design, synthesis, and pharmacological evaluation of novel and selective COX-2 inhibitors based on bumetanide scaffold, Bioorg. Chem. 100 (2020) 103878.
[21] D.L. Namera, S.S. Thakkar, P. Thakor, U. Bhoya, A. Shah, Arylidene analogues as selective COX-2 inhibitors: synthesis, characterization, in silico and *in vitro* studies, J. Biomolecul. Struct. Dyn. (2020) 1–10.
[22] X.-.Q. Yan, Z.-.C. Wang, B. Zhang, P.-.F. Qi, G.-.G. Li, H.-.L. Zhu, Dihydropyrazole derivatives containing benzo oxygen heterocycle and sulfonamide moieties selectively and potently inhibit COX-2: design, synthesis, and anti-colon cancer activity evaluation, Molecules 24 (2019) 1685.
[23] G. Madhava, K.V. Ramana, S.M. Sudhana, D.S. Rao, K.H. Kumar, V. Lokanatha, A.U. Rani, C.N. Raju, Aryl/heteroaryl substituted celecoxib derivatives as COX-2

inhibitors: synthesis, anti-inflammatory activity and molecular docking studies, Med Chem (Los Angeles) 13 (2017) 484–497.
[24] Biovision COX-1 Fluorescent Inhibitor Screening Kit (Catalog No: K548-100) manual.
[25] Biovision COX-2 Fluorescent Inhibitor Screening Kit (Catalog No: K547-100) manual.
[26] D. Osmaniye, B.N. Sağlık, S. Levent, Y. Özkay, Z.A. Kaplancıklı, Design, synthesis and biological evaluation of new N-acyl hydrazones with a methyl sulfonyl moiety as selective COX-2 inhibitors, Chem. Biodivers. (2021) e2100521.
[27] R.G. Kurumbail, A.M. Stevens, J.K. Gierse, J.J. McDonald, R.A. Stegeman, J.Y. Pak, D. Gildehaus, T.D. Penning, K. Seibert, P.C. Isakson, Structural basis for selective inhibition of cyclooxygenase-2 by anti-inflammatory agents, Nature 384 (1996) 644–648.
[28] Maestro, Schrödinger, LLC: New York, NY, USA, (2020).
[29] Schrödinger, LigPrep, Schrödinger, LLC, New York, NY, USA, 2020.
[30] Schrödinger, Glide, Schrödinger, LLC, New York, NY, USA, 2020.
[31] X. Liu, D. Shi, S. Zhou, H. Liu, H. Liu, X. Yao, Molecular dynamics simulations and novel drug discovery, Exp. Opin. Drug Discov. 13 (2018) 23–37.
[32] M.-D.I. Tools, Schrödinger, LLC, New York, NY, 2020, Schrödinger Release 2018-3: Prime, (2018).
[33] B. Sureshkumar, Y.S. Mary, K. Resmi, S. Suma, S. Armaković, S.J. Armaković, C. Van Alsenoy, B. Narayana, D. Sobhana, Spectroscopic characterization of hydroxyquinoline derivatives with bromine and iodine atoms and theoretical investigation by DFT calculations, MD simulations and molecular docking studies, J. Mol. Struct. 1167 (2018) 95–106.
[34] S. Release, 1: Desmond Molecular Dynamics system, Version 3.7, DE Shaw Research, New York, NY, 2014 Maestro-Desmond Interoperability Tools, version, 3.
[35] D.D. Humphreys, R.A. Friesner, B.J. Berne, A multiple-time-step molecular dynamics algorithm for macromolecules, J. Phys. Chem. 98 (1994) 6885–6892.
[36] W.G. Hoover, Canonical dynamics: equilibrium phase-space distributions, Phys. Rev. A 31 (1985) 1695.
[37] G.J. Martyna, D.J. Tobias, M.L. Klein, Constant pressure molecular dynamics algorithms, J. Chem. Phys. 101 (1994) 4177–4189.
[38] U. Essmann, L. Perera, M.L. Berkowitz, T. Darden, H. Lee, L.G. Pedersen, A smooth particle mesh Ewald method, J. Chem. Phys. 103 (1995) 8577–8593.
[39] F.F. Silveira, J.O. de Souza, L.V. Hoelz, V.R. Campos, V.A. Jabor, A.C. Aguiar, M.C. Nonato, M.G. Albuquerque, R.V. Guido, N. Boechat, Comparative study between the anti-P. falciparum activity of triazolopyrimidine, pyrazolopyrimidine and quinoline derivatives and the identification of new PfDHODH inhibitors, Eur. J. Med. Chem. 209 (2021) 112941.
[40] A.M. Mohassab, H.A. Hassan, D. Abdelhamid, A.M. Gouda, H.A. Gomaa, B.G. Youssif, M.O. Radwan, M. Fujita, M. Otsuka, M. Abdel-Aziz, New quinoline/1, 2, 4-triazole hybrids as dual inhibitors of COX-2/5-LOX and inflammatory cytokines: design, Synthesis, and Docking study, J. Mol. Struct. (2021) 130948.
[41] S. Farzaneh, S. Shahhosseini, H. Arefi, B. Daraei, M. Esfahanizadeh, A. Zarghi, Design, synthesis and biological evaluation of new 1, 3-diphenyl-3-(phenylamino) propan-1-ones as selective cyclooxygenase (COX-2) inhibitors, Med. Chem. (Los Angeles) 14 (2018) 652–659.